doi:10.1016/S0022-2836(02)00629-0 available online at http://www.idealibrary.com on IDEAL® J. Mol. Biol. (2002) 321, 411–421

JMB

Chrysanthemum Chlorotic Mottle Viroid RNA: Dissection of the Pathogenicity Determinant and Comparative Fitness of Symptomatic and Non-symptomatic Variants

Marcos De la Peña and Ricardo Flores*

Instituto de Biología Molecular y Celular de Plantas (UPV-CSIC), Avenida de los Naranjos s/n, Universidad Politécnica de Valencia, 46022 Valencia, Spain

Chrysanthemum chlorotic mottle viroid (CChMVd) is a small RNA (398–401 nt) with hammerhead ribozymes in both polarity strands that mediate self-cleavage of the oligomeric RNA intermediates generated in a rolling-circle mechanism of replication. Within the *in vivo* branched RNA conformation of CChMVd, a tetraloop has been identified as a major determinant of pathogenicity. Here we present a detailed study of this tetraloop by site-directed mutagenesis, bioassay of the CChMV-cDNA clones and analysis of the resulting progenies. None of the changes introduced in the tetraloop, including its substitution by a triloop or a pentaloop, abolished infectivity. In contrast to observations for other RNAs, the thermodynamically stable GAAA tetraloop characteristic of non-symptomatic CChMVd-NS strains was not functionally interchangeable for other stable tetraloops of the UNCG family, suggesting that the sequence, rather than the structure, is the major factor governing conservation of this motif. In most cases, the changes introduced initially led to symptomless infections, which eventually evolved to be symptomatic concurrently with the prevalence in the progeny of the UUUC tetraloop characteristic of symptomatic CChMVd-S strains. Only in one case did the GAAA tetraloop emerge and eventually dominate the progeny in infected plants that were non-symptomatic. These results revealed two major fitness peaks in the tetraloop (UUUC and GAAA), whose adjacent stem was also under strong selection pressure. Co-inoculations with CChMVd-S and -NS variants showed that only when the latter was in a 100- or 1000-fold excess did the infected plants remain symptomless, confirming the higher biological fitness of the S variant and explaining the lack of symptom expression previously observed in cross-protection experiments.

Keywords: viroids; RNA structure; tetraloop; hammerhead ribozyme; catalytic RNAs

*Corresponding author

Introduction

Viroids, small single-stranded circular RNAs (between 246 and 401 nt) able to infect certain plants and to incite in most cases pathological alterations, are currently the lowest step of the biological scale.[1,2] As a consequence of their minimal genomic size, viroids are very appropriate systems for the study of RNA structure–function relationships and, specifically, of those involved in pathogenesis. Moreover, since the available evidence indicates that viroids do not code for any protein,[3–5] their pathogenic effects must result from direct interaction of the viroid RNA itself, or of some of its replicative intermediates, with one or more host components. Therefore, viroids also offer unique opportunities to understand how the cellular metabolism can be subverted by a small non-coding RNA.

The 28 viroid species sequenced so far have been grouped within two families. Members of family *Pospiviroidae*, whose type species is *Potato spindle tuber viroid*,[6,7] are characterized for the presence of

Abbreviations used: ASBVd, avocado sunblotch viroid; CChMVd-S and -NS, chrysanthemum chlorotic mottle viroid symptomatic and non-symptomatic, respectively; PLMVd, peach latent mosaic viroid.

E-mail address of the corresponding author: rflores@ibmcp.upv.es

a central conserved region (CCR) and the lack of hammerhead ribozymes, whereas members of family *Avsunviroidae*, whose type species is *Avocado sunblotch viroid* (ASBVd),[8,9] lack a CCR but can form hammerhead structures in both their polarity strands and self-cleave *in vitro* and *in vivo* accordingly.[2,10] Additionally, there is increasing evidence supporting a third demarcating property: whereas the nucleus is the replication and accumulation site of viroids of family *Pospiviroidae*,[11–15] these processes occur in the chloroplast in the case of members of family *Avsunviroidae*.[16–19]

Most studies on sequence or structural determinants of pathogenicity have been carried out with PSTVd and other members of family *Pospiviroidae*, because they were the first discovered and characterized viroids, and also because they usually have herbaceous experimental hosts that make bioassays amenable within a short time interval.[20–24] Studies of this kind have been more limited in the family *Avsunviroidae*, which in addition to ASBVd is composed of *Peach latent mosaic viroid* (PLMVd)[25] and *Chrysanthemum chlorotic mottle viroid* (CChMVd).[26] On the basis of a series of properties that include base composition, overall secondary structure and architecture of the hammerhead ribozymes, PLMVd and CChMVd are related more to each other than to ASBVd and have been grouped in genus *Pelamoviroid*.[2,10,26] The three members of family *Avsunviroidae* are host-specific and have only been experimentally transmitted to other species closely related to their respective natural hosts.[10] Establishing a direct relationship between ASBVd sequence variants and the distinct symptomatology to which they have been associated,[27] is problematic because of the difficulties of achieving successful mechanical inoculations in avocado and the long assay period (approximately one year) required to observe the symptoms. On the other hand, attempts at mapping the pathogenicity determinant(s) of PLMVd have been hampered by the high variability of this viroid as well as by the need to use a woody bioassay host, GF 305 peach seedlings, that still demands a relatively long post-inoculation period of two to three months for symptom expression.[28]

CChMVd offers a much more convenient alternative to this class of studies because its natural host, chrysanthemum, is also a suitable experimental host easy to propagate and with a short time lapse between inoculation and the onset of symptoms (eight to ten days). Moreover, in addition to the severe strains of CChMVd (CChMVd-S), which induces the characteristic chlorotic mottle 2,[26,29,30] the existence of an infectious but non-symptomatic strain of the agent was postulated on the basis of cross-protection studies.[31] Direct proof supporting this contention has recently been provided by cloning and sequencing a CChMVd non-symptomatic strain (CChMVd-NS).[32] By comparative analysis of CChMVd-S and -NS sequence variants and bioassays with natural and site-directed mutagenized CChMVd-cDNA clones, a tetraloop in the thermodynamically most stable branched conformation of CChMVd has been identified as a major determinant of pathogenicity. Furthermore, examination of the sequence heterogeneity found in CChMVd-S and -NS natural variants strongly supports the *in vivo* existence of such a branched conformation, either because the changes are found in loops or because when affecting base-pairs the substitutions are co-variations or compensatory mutations.[32]

Here we report a detailed molecular dissection of this tetraloop by site-directed mutagenesis followed by bioassay of the CChMV-cDNA clones and sequence analysis of the resulting progenies. This sort of *in vivo* evolution experiments provides a powerful tool for the study of RNA structure–function relationships.[33,34] We have also performed a series of *in vivo* competition studies between representative CChMVd-S and -NS variants, using distinct proportions of both competitors in order to determine their relative biological fitness.

Results

The thermodynamically stable GAAA tetraloop characteristic of CChMVd-NS strains is not functionally interchangeable for other stable tetraloops of the UNCG family

A major determinant of pathogenicity for the CChMVd has been mapped in the tetraloop formed by residues 82–85.[32] This tetraloop caps a large stem with a particular secondary structure conserved in the approximately 100 CChMVd variants that we have so far sequenced with only two exceptions: CMNS2 (Ref. 32 and this work), in which a partially different and thermodynamically more stable hairpin can be formed, and CM305VR in which two compensatory insertions extend this stem preserving the rest of its proposed secondary structure (Figure 1).

The sequence of the apical tetraloop between positions 82 and 85 is UUUC for variants obtained from symptomatic strains, as well as UUUU in a few cases (see below), whereas in variants from non-symptomatic strains the sequence of the tetraloop is GAAA, which belongs to the GNRA family of tetraloops (where N is any nucleotide and R a purine residue).[35] Site-directed mutagenesis experiments on the symptomatic CChMVd variant CM20 indicated that the UUUC → GAAA change (generating variant CM20-1), was responsible for viroid pathogenicity.[32] Analysis of ten clones of the progeny resulting from inoculations with CM20-1 revealed that the introduced change and the accompanying non-symptomatic phenotype were stable after three months. In a parallel control experiment in which the symptomatic CM20 variant was inoculated, the phenotype also remained stable after three months and no changes in the

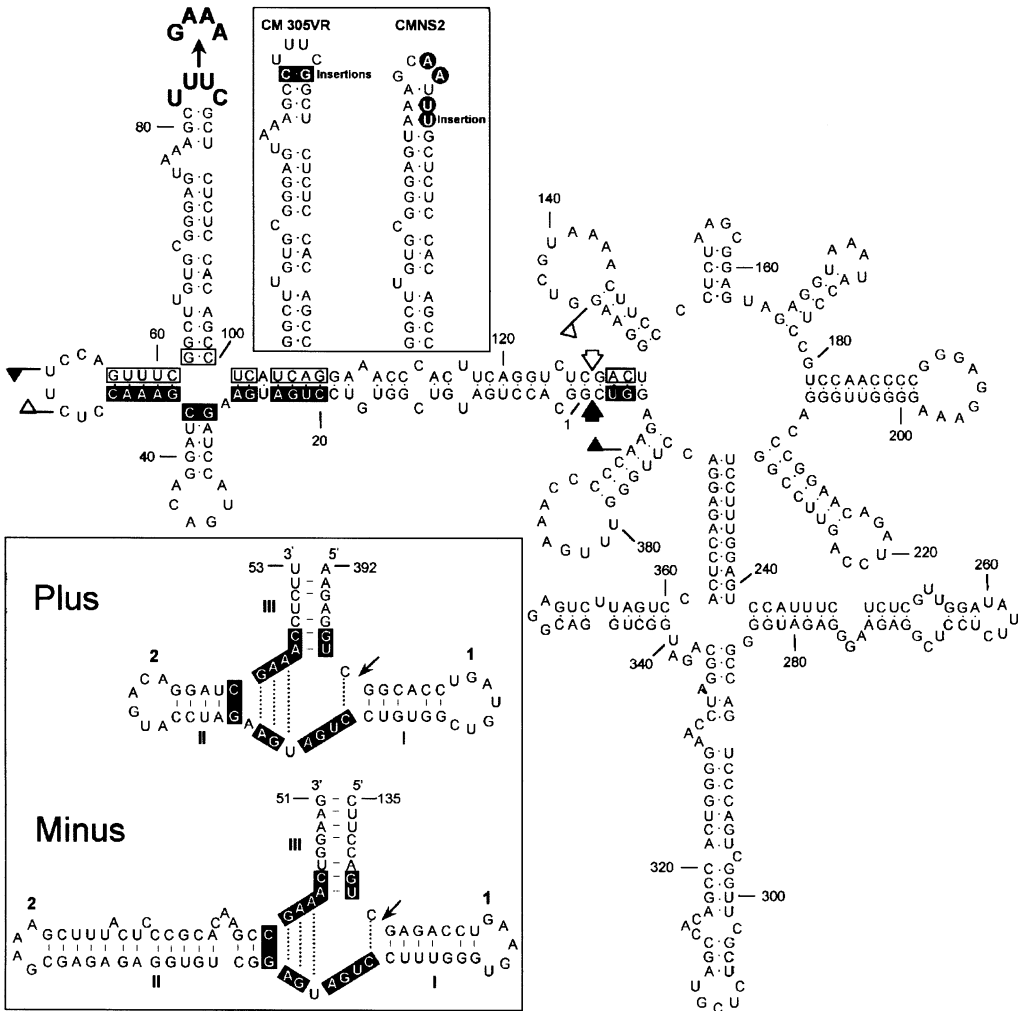

Figure 1. Predicted secondary structure of minimal free energy of the symptomatic CM20 variant. Plus and minus self-cleavage domains are delimited by flags, residues conserved in most natural hammerhead structures are within boxes, and the self-cleavage sites are indicated by arrows. Black and white backgrounds in flags, boxes and arrows refer to plus and minus polarities, respectively. The changes in the tetraloop delimited by positions 82–85 (UUUC → GAAA) that convert a symptomatic variant into non-symptomatic are shown with higher fonts. Upper inset: Characterized variants with changes in the stem-loop structure containing the tetraloop that determines CChMVd pathogenicity. Nucleotide substitutions are indicated in gray background. Lower inset: Hammerhead structures corresponding to the plus and minus polarities of the CChMVd RNA with the residues conserved in most natural hammerhead structures appearing in a black background. Helices and loops are named according to the adopted convention.[44] Continuous and broken lines between bases denote Watson–Crick and non-canonical pairs, respectively.

corresponding tetraloop were observed in the 20 clones sequenced (data not shown).

To gain a deeper insight into the relationships between the 82–85 tetraloop and CChMVd pathogenicity, the effect of site-directed mutations in this tetraloop was studied. At the first attempt, two different tetraloops of the UNCG family (UCCG and UUCG) were introduced into the reference symptomatic clone CM20 to generate recombinant plasmids pCM20-UCCG and pCM20-UUCG. The rationale for this approach was the functional interchangeability, reported previously in some cases, between GNRA and UNCG loops, which have a thermodynamically very stable three-dimensional structure (although the basis for this stability is different), are over-represented in natural RNAs, and have been implicated in many biological functions.[36–38]

When plasmids with the corresponding dimeric head-to-tail inserts pCM20-UCCGd and pCM20-UUCGd were bioassayed in chrysanthemum, no symptoms appeared 15–20 days post-inoculation, when in a parallel control experiment with pCM20d severe symptoms were observed in most inoculated plants. Therefore, both tetraloop changes entailed a reversion of the phenotype from symptomatic to non-symptomatic. One month after inoculation, plants displayed mild symptoms. However, dot-blot analysis revealed that the intensity of the hybridization signals was similar in all cases (including the control plants inoculated with pCM20d), indicating that the

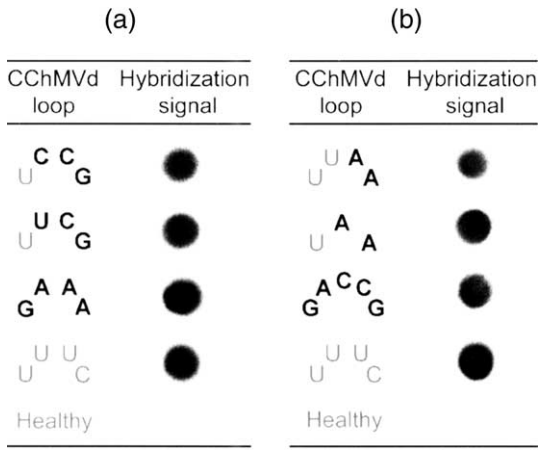

Figure 2. Dot-blot hybridization analysis of chrysanthemum plants inoculated with plasmids containing dimeric CChMVd-cDNA inserts of variants derived from CM20 by site-directed mutagenesis. (a) Results from one experiment in which the tetraloop at positions 82–85 (UUUC) was substituted by UCCG, UUCG and GAAA. (b) Results from a second experiment in which the tetraloop at positions 82–85 (UUUC) was substituted by another tetraloop (UUAA), a triloop (UAA) and a pentaloop (GACCG). Only the tetraloop at positions 82–85 (or its corresponding substitutes) are represented. Bold letters show the changes introduced with respect to the characteristic UUUC symptomatic tetraloop. Plants were analyzed one month after inoculation.

associated phenotypes were not the consequence of different viroid accumulation levels in the infected tissue (Figure 2(a)). However, an initial analysis of the resulting viroid progeny 30 days post-inoculation revealed a high instability of the tetraloop sequences (Figure 3). In none of the obtained cDNA clones was recovered the parental tetraloops but only similar ones. Interestingly, some of the sequences that resulted from the infecting clone with the UCCG tetraloop showed the characteristic UUUC signature of symptomatic variants, involving at least three mutations (two C → U and one G → C). The second most abundant cDNA clone of this progeny had the tetraloop UACA, in which the changes C → A and G → A might indicate an ongoing evolution to a loop similar to that typical of non-symptomatic variants (GAAA). In the case of the sequences derived from the infecting clone with the UUCG tetraloop, some presented the changes C → U and G → U or G → C, giving rise to sequences similar or even identical to the characteristic UUUC tetraloop of symptomatic variants (Figure 3). In fact, the tetraloop of one variant of this progeny (UUUU), was also occasionally found in the progeny of an infectious and symptomatic clone containing the UUUC tetraloop (see below).

Between two and three months after inoculation with pCM20-UCCGd and pCM20-UUCGd, plants showed symptoms of chlorotic mottle. Analysis of the progenies from both parental clones revealed that the tetraloop had reverted to the UUUC characteristic of symptomatic variants, indicating that this is the most abundant tetraloop, if not the only one, in the resulting viroid populations. Altogether these results showed that the thermodynamically stable GAAA tetraloop characteristic of CChMVd-NS strains is not functionally interchangeable for other stable tetraloops of the

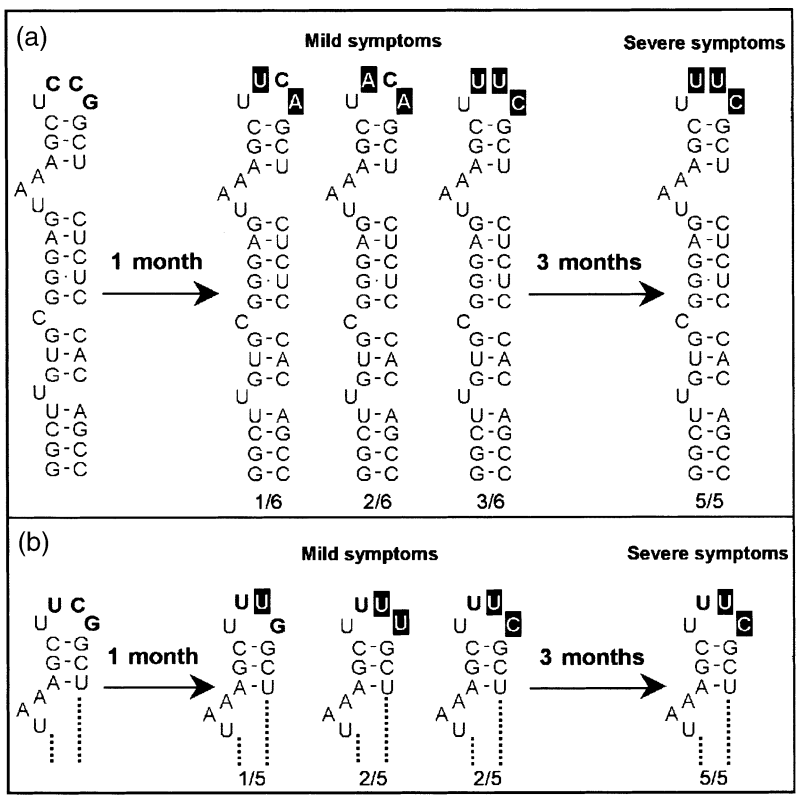

Figure 3. Progeny RNAs from plants inoculated with plasmids containing dimeric CChMVd-cDNA inserts of variants derived from CM20 by site-directed mutagenesis in which the tetraloop at positions 82–85 is UCCG (a) or UUCG (b) (left; only the hairpin capped with the 82–85 tetraloop is represented). The sequences of the resulting progenies (from a representative plant in each case), their relative frequency (indicated by the fractions at the bottom), and the symptoms expressed by the infected plants one and three months after inoculation are presented in the central and right parts, respectively. Bold letters show the changes introduced with respect to the characteristic UUUC symptomatic tetraloop, and white letters on a black background denote spontaneous mutations found in the progenies during the *in vivo* evolution experiments. Other details are as in the legend to Figure 1.

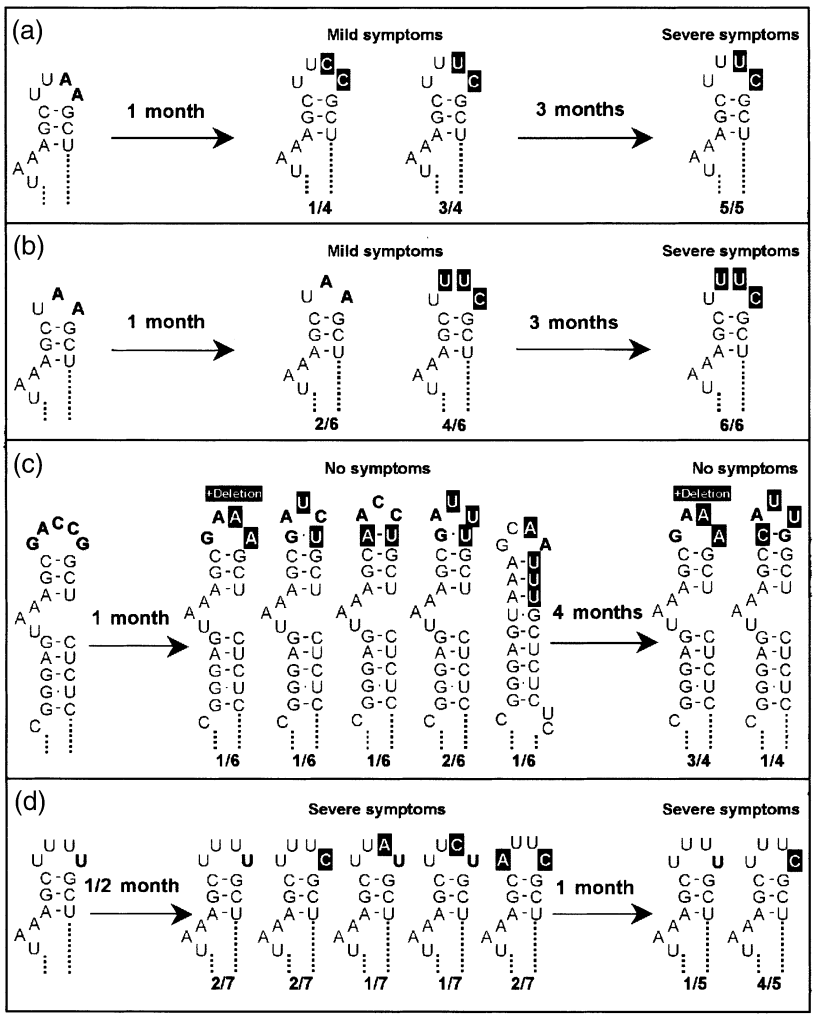

Figure 4. Progeny RNAs from plants inoculated with plasmids containing dimeric CChMVd-cDNA inserts of variants derived from CM20 by site-directed mutagenesis in which the tetraloop at positions 82–85 has been substituted by UUAA (a), UAA (b), GACCG (c) and UUUU (d) (left; only the hairpin capped with the 82–85 tetraloop is represented). The sequences of the resulting progenies (from a representative plant in each case), their relative frequency (indicated by the fractions at the bottom), and the symptoms expressed by the infected plants at two different times after inoculation are presented in the central and right parts, respectively. Bold letters show the changes introduced with respect to the characteristic UUUC symptomatic tetra-loop, and white letters on a black background denote spontaneous mutations found in the progenies during the *in vivo* evolution experiments. Other details are as in the legend to Figure 1.

UNCG family, suggesting that selection pressure acts on the sequence and not on the structure.

Effects of substituting the thermodynamically stable GAAA tetraloop characteristic of CChMVd-NS strains by other tetraloops and by a triloop and a pentaloop

To explore the sequence and size requirements of the tetraloop that determines CChMVd pathogenicity in more detail, we introduced a set of additional changes by site-directed mutagenesis at this tetraloop, and the recombinant plasmids with the corresponding dimeric head-to-tail inserts were bioassayed in chrysanthemum. As a first step, the effect of introducing the "hybrid" tetraloop UUAA (a combination of the UUUC and GAAA tetraloops characteristic of CChMVd-S and -NS strains, respectively) was studied. One month after inoculation, the viroid progeny showed changes in only the 3′-half of the tetraloop, with most of the sequences reverting to the typical symptomatic UUUC tetraloop, an observation consistent with the appearance of mild symptoms in the infected plants (Figure 4(a)). Three months after inoculation these symptoms had evolved to severe and, concurrently, only variants with the UUUC tetraloop were detected from the progeny (Figure 4(a)).

An analogous situation was found when bioassays were performed with dimeric constructs containing the UAA triloop. The inoculated plants displayed mild symptoms one month after inoculation and only two types of sequences, the parental UAA and, predominating, the UUUC characteristic of the symptomatic strain, were detected in the resulting progeny (Figure 4(b)). Three months after inoculation all plants expressed severe symptoms and, again, only variants with the UUUC tetraloop were detected from the progeny (Figure 4(b)).

In a third experiment, a pentaloop with the sequence GACCG was introduced. The two 5′-terminal nucleotides were identical to those in similar positions in the characteristic non-symptomatic GAAA tetraloop, whereas the 3′-moiety neither resembled this nor the UUUC tetraloop typical of the symptomatic strain. One month after inoculation with the corresponding dimeric construct all plants were infected but expressed no symptoms. The original pentaloop was not preserved in any of the analysed variants from the

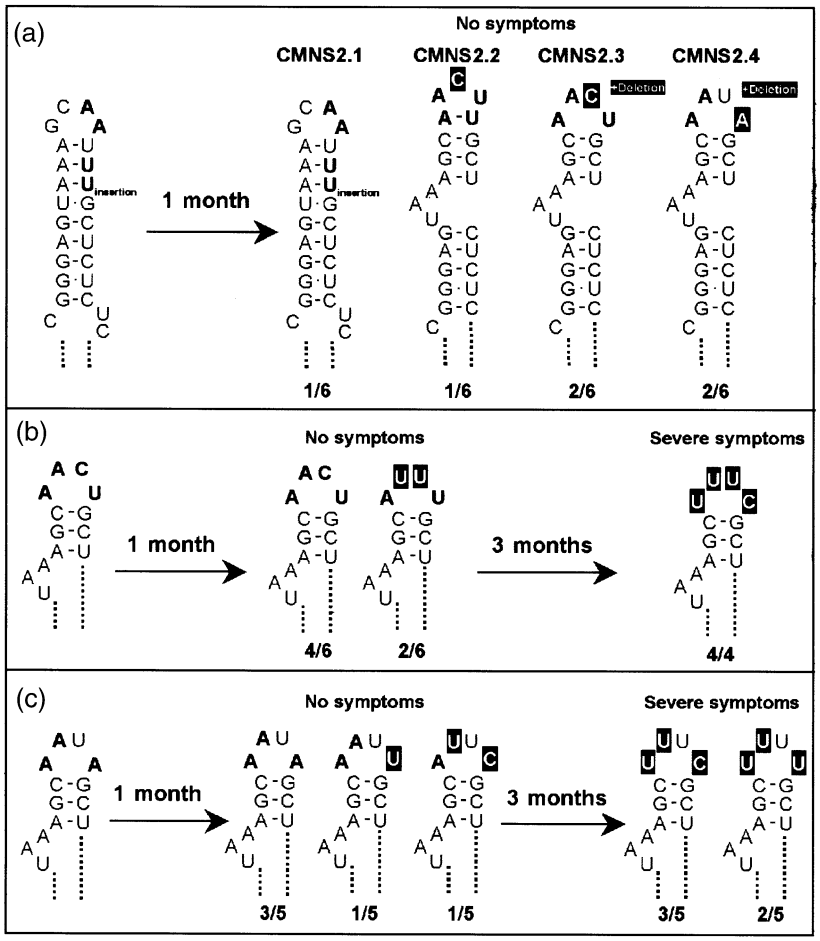

Figure 5. Progeny RNAs from plants inoculated with plasmids containing dimeric CChMVd-cDNA inserts of natural variants CMNS 2 (a), 2.3 NS (b) and 2.4 NS (c) (left; only the hairpin capped with the 82–85 tetraloop is represented). The sequences of the resulting progenies (from a representative plant in each case), their relative frequency (indicated by the fractions at the bottom), and the symptoms expressed by the infected plants at different times after inoculation are presented in the central and right parts, respectively. Bold letters show the changes with respect to the characteristic UUUC symptomatic tetraloop, and white letters on a black background denote spontaneous mutations found in the progenies during the *in vivo* evolution experiments. Other details are as in the legend to Figure 1.

resulting progeny; one of them, however, had the characteristic non-symptomatic GAAA tetraloop, another could form a hairpin identical to that of the natural variant CMNS2 previously obtained from a non-symptomatic isolate,[32] and others presented changes allowing the formation of a triloop (Figure 4(c)). The infected plants remained symptomless after four months, and a limited analysis of the progeny at this time revealed only two types of variants: three had the characteristic non-symptomatic GAAA tetraloop, and one presented a new sequence (CAUUG) that in the thermodynamically most stable secondary structure could form a triloop closed by a C–G pair (Figure 4(c)). In the last experiment of this series, the UUUC tetraloop typical of the symptomatic strain was changed into the closely related UUUU previously found in the progeny of CChMVd variant CM1 (Ref. 26 and data not shown). As soon as 15 days post-inoculation all plants showed severe symptoms, indicating an infectivity and pathogenicity similar to that of variants with the UUUC tetraloop. Analysis of the resulting progeny showed a predominance of variants with the parental UUUU and the symptomatic UUUC tetraloops (Figure 4(d)). One month after inoculation, these plants remained symptomatic but the progeny showed a clear prevalence of variants with the UUUC tetraloop (Figure 4(d)). In all, these results corroborated the high selection pressure which exists at this region that favors the prevalence of two tetraloops (UUUC and to a lesser extent UUUU). In these four experiments dot-blot analysis failed to detect significant differences in the accumulation level of the viroid progeny (Figure 2(b), data not shown), indicating that this is not the factor determining the observed phenotypes.

Genetic stability of a natural non-symptomatic CChMVd variant with an atypical stem-tetraloop in the region involved in pathogenicity

In the course of the characterization of a CChMVd-NS strain, a variant (CMNS2) with some peculiarities in the region containing the tetraloop that determines CChMVd pathogenicity was found.[32] This variant presented four distinct mutations between positions 80 and 86, but distributed in such a way that they allowed the adoption of a hairpin stem of nine uninterrupted base-pairs capped with a different tetraloop (GCAA) of the GNRA family (Figure 5(a)). Interestingly, a variant with the same stem–tetraloop hairpin was characterized in the progeny resulting from the infection with the construct containing the GACCG pentaloop (Figure 4(c)). To assess the genetic stability of the CMNS2 variant, a recombinant plasmid with

Table 1. Effects of co-inoculations with CChMVd symptomatic (S) and non-symptomatic (NS) variants on viroid progeny and symptom expression of chrysanthemum plants

Ratio of S to NS variants in inocula[a]	S and NS variants in the progeny (15 days p.i.)	Symptoms (15 days p.i.)
1:1	9 and 3[b]	Mild (4/4)[c]
10:1	10 and 0	Severe (4/4)
1:10	8 and 4	Mild (2/4)
	1 and 8	None (2/4)
Control (only S variant)	6 and 0	Severe (4/4)
Control (only NS variant)	0 and 8	None[d]
Buffer	None	None

[a] S and NS refer to the symptomatic (CM20) and non-symptomatic (CM20-1) variants, respectively.
[b] Number of variants in the progeny from one of the infected plants with the tetraloops characteristic of symptomatic and non-symptomatic variants.
[c] Number of plants with symptoms with respect to those inoculated (four plants with each inoculum).
[d] All inoculated plants were infected as revealed by dot-blot analysis.

the corresponding dimeric insert was bioassayed in chrysanthemum. One month after inoculation, dot-blot hybridization revealed that although all plants were infected and accumulating similar viroid levels (data not shown), they were symptomless, and analysis of the progeny showed a considerable variability in the region encompassing the tetraloop. Only one of the six recovered variants had the parental hairpin preserved, whereas the others presented different mutations that restored the common hairpin stem with three bulging residues (Figure 5(a)).

Two of the variants from the CMNS2 progeny had the tetraloops AACU and AAUA in the region that determines CChMVd pathogenicity. To study whether these tetraloops evolved in similar or different directions, recombinant plasmids with dimeric cDNA inserts of both variants were independently bioassayed. One month after the inoculation with the variant containing the AACU tetraloop all plants were infected but symptomless, and the viroid progeny was composed of a mixture of two tetraloop sequences: the parental and another with the change AACU → AUUU (Figure 5(b)). However, three months after inoculation some plants expressed severe symptoms and an analysis of the viroid population showed a reversion to the typical symptomatic UUUC tetraloop (Figure 5(b)). In a parallel way, one month after inoculation with the variant containing the AAUA tetraloop all plants were infected but symptomless, and the viroid progeny was composed of a mixture of tetraloop sequences in which the parental was predominant (Figure 5(c)). Three months after inoculation a fraction of the plants expressed severe symptoms and the viroid population was composed of variants with the symptomatic UUUC and UUUU tetraloops (Figure 5(c)). As in the previous experiments, dot-blot hybridization revealed no significant differences in the accumulation level of the viroid progeny (data not shown). Collectively, these results indicated that there is a strong selection pressure not only on the tetraloop but also on the structure of the adjacent stem, and that the symptomatic and non-symptomatic variants have a differential biological fitness (with the first being more efficient than the second).

Co-inoculation experiments of CChMVd variants show a relationship between pathogenicity and biological fitness

To provide additional support for the higher fitness of the symptomatic variant, gel-purified monomeric RNAs, resulting from self-cleavage during *in vitro* transcription of plasmids with dimeric symptomatic and non-symptomatic CChMVd-cDNA inserts, were co-inoculated at different proportions in chrysanthemum plants. In a first experiment, the symptomatic variant CM20 (UUUC, positions 82–85) and its non-symptomatic derivative CM20-1 (UUUC → GAAA), were chosen for the competition assays. Taking advantage of the fact that residues at positions 82–83 in the symptomatic cDNA clones form part of a *Hin*dIII site (AAGCTT, positions 78–83), the proportion of both competitors in the progeny was easily determined by restriction analysis.[32] Control inoculations with either of the variants and sequencing of several cDNA clones of the resulting progenies confirmed the genetic stability of both UUUC and GAAA tetraloops and of their associated phenotypes (Table 1). When equimolecular amounts of both competitors were co-inoculated, variants with the UUUC tetraloop predominated over those with the GAAA tetraloop (in a ratio 3:1), and plants displayed a mild symptomatology. When the symptomatic variant was in a tenfold excess in the inoculum, only the UUUC tetraloop was detected in the progeny and plants displayed severe symptoms. In contrast, when the non-symptomatic variant was tenfold more abundant in the inoculum than the symptomatic, half the plants exhibited a mild phenotype and two-thirds of the recoverd clones had the UUUC tetraloop; the other half had no symptoms and the GAAA tetraloop was prevalent in the progeny (in a ratio 8:1) (Table 1). These results showed that the symptomatology observed could be directly related to the

proportion of both types of variants in the progeny, and that the biological fitness of the symptomatic variant was significantly higher than that of its non-symptomatic counterpart.

In a second competition experiment, the symptomatic variant was the same as in the first experiment but the non-symptomatic was CMNS35, a natural variant in which the UUUC → GAAA change is accompanied by other mutations outside the tetraloop.[32] When the co-inoculations were performed with monomeric RNA mixtures from both variants in the proportions 1:1, 10:1 and 1:10, the symptom expression pattern in the infected plants 15–20 days post-inoculation was very similar to that of the previous experiment (data not shown). Only in co-inoculations in which the non-symptomatic variant was in 100- or 1000-fold excess, did all plants remain symptomless for two months after inoculation (although dot-blot analysis showed that they were infected). These results confirmed the greater biological fitness of the symptomatic variant, and explain the lack of symptom expression observed in plants inoculated in a cross-protection format (Refs. 31,32 and see also Discussion).

Discussion

Within family *Avsunviroidae*, CChMVd represents the best choice for reverse genetics studies on structural–functional relationships mainly because chrysanthemum is easily propagated from cuttings in the greenhouse, and reacts to infection with plasmids containing dimeric cDNA inserts of the viroid with diagnostic symptoms in a relatively short time. Using this system, we have shown that the CChMVd pathogenicity determinant maps to a tetraloop in the branched conformation of the viroid,[32] and that the plus hammerhead ribozyme of CChMVd deviates from the consensus catalytic core due to the involvement of an extra residue in critical function(s) other than self-cleavage.[39] Here we have focused our attention on the tetraloop that determines patogenicity in an attempt to get a deeper insight into it and into the mechanism underlying cross-protection phenomena in CChMVd.

One striking observation of our experiments is that none of the changes introduced by site-directed mutagenesis in the tetraloop involved in CChMVd pathogenicity abolished infectivity, even in those cases in which the tetraloop was substituted by a triloop or a pentaloop. This is not a general situation in CChMVd as we previously reported that the deletion of a single residue (A27 in the CChMVd reference sequence) annuls infectivity,[39] indicating that selection pressures of very different intensity operate in distinct regions of the viroid molecule. A second observation is that in contrast with what is known about other RNAs,[38] but in line with what has been observed for the RNA of potato virus X,[40] the thermodynamically stable GAAA tetraloop characteristic of CChMVd-NS strains is not functionally interchangeable for other stable tetraloops of the UNCG family, suggesting that it is the sequence, rather than the structure, that is the major factor governing the preservation of this motif. In most cases, the changes introduced in this tetraloop led initially to symptomless infections, that eventually evolved to symptomatic concurrently with the appearance and prevalence in the resulting progeny of the UUUC tetraloop characteristic of CChMVd-S strains (Figures 3 and 4). This was also the case of the two bottleneck experiments in which two variants from the CMNS2 progeny were used (Figure 5(b) and (c)). Therefore, the symptomatic phenotype is associated with one or a very reduced number of sequences (UUUU would be the second and less important example) in this region of the viroid molecule. Only in the case in which the infecting variant had the GACCG pentaloop, with the same two 5′-terminal nucleotides as the GAAA tetraloop characteristic of CChMVd-NS strains, did this latter tetraloop emerge and eventually dominate the progeny. This clearly shows that the adaptative landscape of CChMVd has two major fitness peaks in the region delimited by positions 82–85 that correspond to variants with UUUC and GAAA tetraloops.

The secondary structure of the stem capped by these tetraloops is also under strong selection pressure, as revealed by bioassays with the non-symptomatic variant CMNS2. Only one month after inoculation, the infecting variant was almost outcompeted by new ones in which the CMNS2 hairpin stem of nine uninterrupted base-pairs was substituted by the characteristic stem with three bulging residues (Figure 5). These results indicate that despite the existence in progenies from natural (CMNS2) and artificial variants (those with the GACCG pentaloop) of sequences with an alternative conformation for the hairpin stem-loop between positions 71 and 93, they are not maintained and rapidly evolved to the standard type by accumulation of point mutations and deletions in the AAUUU region. Also in this context it should be noted that an additional selection pressure could operate as a consequence of the fact that the tetraloop which determines CChMVd pathogenicity and its adjacent stem, form loop 2 and helix II of the minus hammerhead structure, respectively (Figure 1). Although loop 2, due to the length of helix II, would appear to be located far away from the catalytic core of the ribozyme, bending of helix II caused by its bulging residues might facilitate the interaction of loop 2 with other structural elements of the ribozyme, particularly with helix I-loop 1.

The co-inoculation experiments using typical CChMVd-S and -NS variants at different proportions confirmed the higher biological fitness of the symptomatic variant. Only when the non-symptomatic variant was in a tenfold excess in the

inoculum, did a fraction of the plants remain symptomless, whereas when the excess was 100- or 1000-fold, all plants, although infected, did not express symptoms (Table 1). These results are consistent with the protection afforded by CChMVd-NS strains against their S counterparts when inoculated in a cross-protection format.[31,32] Cross-protection phenomena refer to the observation that viroid ability to infect a host plant may relate to previous infections by other strains of the same or by a closely related viroid. In fact, when a plant is pre-infected with a mild viroid strain and is then challenge-inoculated with a severe strain of the same viroid, the typical symptoms of the second strain and the accumulation level of its corresponding RNA are attenuated for an uncertain period of time, probably as a consequence of the competition between the two RNAs for a limiting host factor. On this basis, the existence of CChMVd-NS strains was first postulated, even before CChMVd was identified as a viroid, to explain why some plants of a chrysanthemum cultivar sensitive to the disease were unable to develop the characteristic symptoms when inoculated with extracts from a CChMVd-S strain.[31] The present results show that CChMVd-NS variants, with a characteristic GAAA tetraloop in positions 82–85 (Ref. 32 and data not shown), can also efficiently protect against CChMVd-S variants in a co-inoculation format, provided that the inoculum contains a vast excess of the former over the latter.

Materials and Methods

Viroid strains and extraction of viroid RNA

Most variants were obtained of the CChMVd-S and -NS strains characterized previously in the chrysanthemum cultivars "Bonnie Jean" and "Yellow Delaware", respectively.[26,32] A minor fraction of the variants were obtained from a CChMVd-S strain infecting the cultivar "Velvet Ridge" (they are referred with the letters VR in their names). For dot-blot hybridization, RNAs from chrysanthemum leaves (2 g) were extracted with buffer-saturated phenol and fractionated on non-ionic cellulose (CF11, Whatman), which was washed with STE (50 mM Tris–HCl, 100 mM NaCl, 1 mM EDTA, pH 7.2) containing 35% (v/v) ethanol and then with STE.[41]

Infectivity bioassays and detection of viroid RNA

Chrysanthemum (*Dendranthema grandiflora* Tzvelez, cv. Bonnie Jean) was propagated in growth chambers.[26] Plants were mechanically inoculated with recombinant plasmids containing dimeric head-to-tail CChMVd-cDNA inserts (2 μg of plasmid per plant), or with their corresponding monomeric CChMVd RNAs resulting from self-cleavage during *in vitro* transcription. CChMVd infection was assessed by dot-blot hybridization with a radioactive full-length RNA probe complementary to the CChMVd-S variant CM20 obtained by transcription with T7 RNA polymerase of a linearized recombinant plasmid.[32]

Co-inoculation experiments

The recombinant plasmids pCM20d, pCM20.1d and pCM35NSd, containing the head-to-tail dimeric cDNA inserts of CChMVd variants CM20, CM20.1 and CM35NS, respectively, were linearized with *Eco* RI and *in vitro* transcribed with T7 RNA polymerase.[42] The primary transcripts of (+) polarity and their self-cleavage products were separated by PAGE in 5% (w/v) gels containing 1 × TBE and 8 M urea, and the RNAs of monomeric length were eluted and quantified. Co-inoculations were performed by mixing appropriate amounts of monomeric RNAs of the symptomatic and non-symptomatic variants to obtain 1:1, 1:10, 1:100 and 1:1000 ratios; each plant was mechanically inoculated with approximately 1 μg of total RNA.

Progeny analysis by RT-PCR amplification, cloning, and sequencing

Viroid circular forms purified by two consecutive PAGE steps, were reverse-transcribed and PCR-amplified with the pair of adjacent primers PIII (complementary to nucleotides 133–108) and PIV (homologous to nucleotides 134–159) of the CM20 variant obtained from CChMVd-S strain (see Figure 1). Reverse transcription, PCR amplification (with *Pfu* DNA polymerase (Stratagene), endowed with proof-reading activity), and cloning were performed as described.[32] Inserts were sequenced automatically with an ABI Prism DNA sequencer (Perkin–Elmer).

Site-directed mutagenesis

A PCR-based protocol[43] was followed with minor modifications. Plasmid pCM20 (5 ng) was amplified with 250 ng each of pairs of adjacent and phosphorylated primers complementary and homologous to nucleotides 57–83 and 84–112 of the CM20 variant, respectively, with the exception of the first two 5′ positions of each primer in which appropriate changes were introduced to obtain different tetra- tri- and pentaloops (GAAA, UCCG, UUCG, UUAA, UUUU, UAA, and GACCG) in the region delimited by positions 82–85 (Figure 1). The PCR cycling profile, designed to amplify the complete plasmids with *Pfu* DNA polymerase, was the same reported previously.[32] After electrophoresis in agarose gels, PCR products of plasmid length were eluted, circularized with T4 DNA ligase, and used for transformation. Sequencing confirmed that the new plasmids contained solely the expected mutations.

Acknowledgments

We are grateful to A. Ahuir for taking care of the plants and for technical assistance, and to Dr R. K. Horst for CChMVd strains. This work was partially supported by grant PB98-0500 (to R.F.) from the DGES de España. M.D.P. was the recipient of a pre-doctoral fellowship from the Ministerio de Ciencia y Tecnología de España.

References

1. Diener, T. O. (2001). The viroid: biological oddity or evolutionary fossil? *Advan. Virus Res.* **57**, 137–184.

2. Flores, R., Randles, J. W., Bar-Joseph, M. & Diener, T. O. (2000). Viroids. In *Virus Taxonomy: Seventh Report of the International Committee on Taxonomy of Viruses* (van Regenmortel, M. H. V., Fauquet, C. M., Bishop, D. H. L., Carstens, E. B., Estes, M. K., Lemon, S. M., Maniloff, J., Mayo, M. A., McGeoch, D. J., Pringle, C. R. & Wickner, R. B., eds), pp. 1009–1024, Academic Press, San Diego.
3. Davies, J. W., Kaesberg, P. & Diener, T. O. (1974). Potato spindle tuber viroid XII. An investigation of viroid RNA as a messenger for protein synthesis. *Virology*, **61**, 281–286.
4. Hall, T. C., Wepprich, R. K., Davies, J. W., Weathers, L. G. & Semancik, J. S. (1974). Functional distinctions between the ribonucleic acids from citrus exocortis viroid and plant viruses: cell-free translation and aminoacylation reactions. *Virology*, **61**, 486–492.
5. Semancik, J. S., Conejero, V. & Gerhart, J. (1977). Citrus exocortis viroid: survey of protein synthesis in *Xenopus laevis* oocytes following addition of viroid RNA. *Virology*, **80**, 218–221.
6. Diener, T. O. (1972). Potato spindle tuber viroid VIII. Correlation of infectivity with a UV-absorbing component and thermal denaturation properties of the RNA. *Virology*, **50**, 606–609.
7. Gross, H. J., Domdey, H., Lossow, C., Jank, P., Raba, M., Alberty, H. & Sänger, H. L. (1978). Nucleotide sequence and secondary structure of potato spindle tuber viroid. *Nature*, **273**, 203–208.
8. Symons, R. H. (1981). Avocado sunblotch viroid: primary sequence and proposed secondary structure. *Nucl. Acids Res.* **9**, 6527–6537.
9. Hutchins, C., Rathjen, P. D., Forster, A. C. & Symons, R. H. (1986). Self-cleavage of plus and minus RNA transcripts of avocado sunblotch viroid. *Nucl. Acids Res.* **14**, 3627–3640.
10. Flores, R., Daròs, J. A. & Hernández, C. (2000). The *Avsunviroidae* family: viroids with hammerhead ribozymes. *Advan. Virus Res.* **55**, 271–323.
11. Diener, T. O. (1971). Potato spindle tuber virus: a plant virus with properties of a free nucleic acid. III. Subcellular location of PSTV-RNA and the question of whether virions exist in extracts or *in situ*. *Virology*, **43**, 75–89.
12. Spiesmacher, E., Mühlbach, H. P., Schnölzer, M., Haas, B. & Sänger, H. L. (1983). Oligomeric forms of potato spindle tuber viroid (PSTV) and of its complementary RNA are present in nuclei isolated from viroid-infected potato cells. *Biosci. Rep.* **3**, 767–774.
13. Harders, J., Lukacs, N., Robert-Nicoud, M., Jovin, J. M. & Riesner, D. (1989). Imaging of viroids in nuclei from tomato leaf tissue by *in situ* hybridization and confocal laser scanning microscopy. *EMBO J.* **8**, 3941–3949.
14. Bonfiglioli, R. G., Webb, D. R. & Symons, R. H. (1996). Tissue and intra-cellular distribution of coconut cadang cadang viroid and citrus exocortis viroid determined by *in situ* hybridization and confocal laser scanning and transmission electron microscopy. *Plant J.* **9**, 457–465.
15. Woo, Y.-M., Itaya, A., Owens, R. A., Tang, L., Hammons, R. W., Chou, H.-C. *et al.* (1999). Characterization of nuclear import of potato spindle tuber viroid RNA in permeabilized protoplasts. *Plant J.* **17**, 627–635.
16. Bonfiglioli, R. G., McFadden, G. I. & Symons, R. H. (1994). *In situ* hybridization localizes avocado sunblotch viroid on chloroplast thylakoid membranes and coconut cadang cadang viroid in the nucleus. *Plant J.* **6**, 99–103.
17. Lima, M. I., Fonseca, M. E. N., Flores, R. & Kitajima, E. W. (1994). Detection of avocado sunblotch viroid in chloroplasts of avocado leaves by *in situ* hybridization. *Arch. Virol.* **138**, 385–390.
18. Bussière, F., Lehoux, J., Thompson, D. A., Skrzeczkowski, L. J. & Perreault, J. P. (1999). Subcellular localization and rolling circle replication of peach latent mosaic viroid: hallmarks of group A viroids. *J. Virol.* **73**, 6353–6360.
19. Navarro, J. A., Daròs, J. A. & Flores, R. (1999). Complexes containing both polarity strands of avocado sunblotch viroid: identification in chloroplasts and characterization. *Virology*, **253**, 77–85.
20. Schnölzer, M., Haas, B., Ramm, K., Hofmann, H. & Sänger, H. L. (1985). Correlation between structure and pathogenicity of potato spindle tuber viroid (PSTV). *EMBO J.* **4**, 2181–2190.
21. Visvader, J. E. & Symons, R. H. (1986). Replication of *in vitro* constructed viroid mutants: location of the pathogenicity-modulating domain in citrus exocortis viroid. *EMBO J.* **13**, 2051–2055.
22. Owens, R. A., Steger, G., Hu, Y., Fels, A., Hammond, R. W. & Riesner, D. (1996). RNA structural features responsible for potato spindle tuber viroid pathogenicity. *Virology*, **222**, 144–158.
23. Reanwarakorn, K. & Semancik, J. S. (1998). Regulation of pathogenicity in hop stunt viroid-related group II citrus viroids. *J. Gen. Virol.* **79**, 3163–3171.
24. Schmitz, A. & Riesner, D. (1998). Correlation between bending of the VM region and pathogenicity of different potato spindle tuber viroid strains. *RNA*, **4**, 1295–1303.
25. Hernández, C. & Flores, R. (1992). Plus and minus RNAs of peach latent mosaic viroid self-cleave *in vitro via* hammerhead structures. *Proc. Natl Acad. Sci. USA*, **89**, 3711–3715.
26. Navarro, B. & Flores, R. (1997). Chrysanthemum chlorotic mottle viroid: unusual structural properties of a subgroup of viroids with hammerhead ribozymes. *Proc. Natl Acad. Sci. USA*, **94**, 11262–11267.
27. Semancik, J. S. & Szychowski, J. A. (1994). Avocado sunblotch disease: a persistent viroid infection in which variants are associated with differential symptoms. *J. Gen. Virol.* **75**, 1543–1549.
28. Ambrós, S., Hernández, C., Desvignes, J. C. & Flores, R. (1998). Genomic structure of three phenotypically different isolates of peach latent mosaic viroid: implications of the existence of constraints limiting the heterogeneity of viroid quasi-species. *J. Virol.* **72**, 7397–7406.
29. Romaine, C. P. & Horst, R. K. (1975). Suggested viroid etiology for chrysanthemum chlorotic mottle disease. *Virology*, **64**, 86–95.
30. Horst, R. K. (1987). Chrysanthemum chlorotic mottle. In *The Viroids* (Diener, T. O., ed.), pp. 291–295, Plenum, New York.
31. Horst, R. K. (1975). Detection of a latent infectious agent that protects against infection by chrysanthemum chlorotic mottle viroid. *Phytopathology*, **65**, 1000–1003.
32. De la Peña, M., Navarro, B. & Flores, R. (1999). Mapping the molecular determinat of pathogenicity in a hammerhead viroid: a tetraloop within the *in vivo* branched RNA conformation. *Proc. Natl Acad. Sci. USA*, **96**, 9960–9965.

33. Olsthoorn, R. C. L., Licis, N. & Van Duin, J. (1994). Leeway and constraints in the forced evolution of a regulatory RNA helix. *EMBO J.* **13**, 2660–2668.
34. Miller, E. D., Kim, K.-H. & Hemenway, C. (1999). Restoration of a stem-loop structure required for potato virus X accumulation indicates selection for a mismatch and a GNRA tetraloop. *Virology*, **260**, 342–353.
35. Heus, H. A. & Pardi, A. (1991). Structural features that give rise to the unusual stability of RNA hairpins containing GNRA loops. *Science*, **253**, 191–194.
36. Woese, C. R., Winker, S. & Gutell, R. R. (1990). Architecture of ribosomal RNA: constraints on the sequence of tetra-loops. *Proc. Natl Acad. Sci. USA*, **87**, 8467–8471.
37. Cheong, C., Varani, G. & Tinoco, I., Jr (1990). Solution structure of an unusually stable RNA hairpin, 5′GGAC(UUCG)GUCC3′. *Nature*, **346**, 680–682.
38. Selinger, D., Xiubei, L. & Wise, J. A. (1993). Functional interchangeability of the structurally similar tetranucleotide loops GAAA and UUCG in fission yeast signal recognition particle RNA. *Proc. Natl Acad. Sci. USA*, **90**, 5409–5413.
39. De la Peña, M. & Flores, R. (2001). An extra nucleotide in the consensus catalytic core of a viroid hammerhead ribozyme: implications for the design of more efficient ribozymes. *J. Biol. Chem.* **276**, 34586–34593.
40. Miller, E. D., Plante, C. A., Kim, K.-H., Brown, J. W. & Hemenway, C. (1998). Stem-loop structure in the 5′ region of potato virus X genome required for plus strand RNA accumulation. *J. Mol. Biol.* **284**, 591–608.
41. Pallás, V., Navarro, A. & Flores, R. (1987). Isolation of a viroid-like RNA from hop different from hop stunt viroid. *J. Gen. Virol.* **68**, 2095–2102.
42. Forster, A. C., Davies, C., Hutchins, C. J. & Symons, R. H. (1990). Characterization of self-cleavage of viroids and virusoid RNAs. *Methods Enzymol.* **181**, 583–607.
43. Byrappa, S., Gavin, D. K. & Gupta, K. C. (1995). A highly efficient procedure for site-specific mutagenesis of full-length plasmids using *Vent* DNA polymerase. *PCR Methods Appl.* **5**, 404–407.
44. Hertel, K. J., Pardi, A., Uhlenbeck, O. K., Koizumi, M., Ohtsuka, E., Uesugi, S. *et al.* (1992). Numbering system for the hammerhead. *Nucl. Acids Res.* **20**, 3252.

Edited by D. E. Draper

(Received 15 March 2002; received in revised form 18 June 2002; accepted 20 June 2002)